HBRC Journal (2016) 12, 33–46

Housing and Building National Research Center

HBRC Journal

http://ees.elsevier.com/hbrcj

Experimental and analytical investigation of the lateral load response of confined masonry walls

Hussein Okail [1], Amr Abdelrahman [2], Amr Abdelkhalik [*,3], Mostafa Metwaly [3]

Structural Engineering Department, Ain Shams University, Cairo, Egypt

Received 7 May 2014; revised 17 August 2014; accepted 2 September 2014

KEYWORDS

Confined masonry;
Infilled frames;
Seismic behavior;
Lateral loads;
Shear failure

Abstract This paper investigates the behavior of confined masonry walls subjected to lateral loads. Six full-scale wall assembles, consisting of a clay masonry panel, two confining columns and a tie beam, were tested under a combination of vertical load and monotonic pushover up to failure. Wall panels had various configurations, namely, solid and perforated walls with window and door openings, variable longitudinal and transverse reinforcement ratios for the confining elements and different brick types, namely, cored clay and solid concrete masonry units. Key experimental results showed that the walls in general experienced a shear failure at the end of the lightly reinforced confining elements after the failure of the diagonal struts formed in the brick wall due to transversal diagonal tension. Stepped bed joint cracks formed in the masonry panel either diagonally or around the perforations. A numerical model was built using the finite element method and was validated in light of the experimental results. The model showed acceptable correlation and was used to conduct a thorough parametric study on various design configurations. The conducted parametric study involved the assessment of the load/displacement response for walls with different aspect ratios, axial load ratios, number of confining elements as well as the size and orientation of perforations. It was found that the strength of the bricks and the number of confining elements play a significant role in increasing the walls' ultimate resistance and displacement ductility.

* Corresponding author. Tel.: +20 1008444069.
E-mail address: amr_civileng@yahoo.com (A. Abdelkhalik).
[1] Assistant Professor.
[2] Professor.
[3] Research Assistant.

Peer review under responsibility of Housing and Building National Research Center.

Production and hosting by Elsevier

Introduction

Confined masonry (CM) is considered one of the popular forms of low-cost, low-rise constructions throughout the world; including the Middle East, South and Central America, Mexico, South-East Asia, and South-Eastern Europe [1]. The system relies on a load-bearing wall encased by small cast-in-place reinforced concrete tie columns and tie beams [2,3]. The distinguishing feature of confined masonry construction is that the masonry wall is constructed prior to the casting of

http://dx.doi.org/10.1016/j.hbrcj.2014.09.004
1687-4048 © 2014 Production and hosting by Elsevier B.V. on behalf of Housing and Building National Research Center.

the confining elements, tie columns and tie beams, thus both elements respond integrally when subjected to lateral loads in addition to the cost reduction of the formwork. In general, tie columns have a rectangular section whose dimensions typically correspond to the wall thickness. For tie beams, both wall thickness and floor type influence the choice of the dimensions. The confining elements are intended to confine the masonry panel preventing disintegration, to enhance wall deformation capacity, and connectivity with other walls and floor diaphragms. The recent European codes state that the contribution of vertical confinement to vertical and lateral resistance should be ignored [4]. The amount of reinforcement is determined empirically on the basis of experience, and depends on the height and size of the building.

In a way, the behavior is similar to that of infilled reinforced concrete frames. However, in the case of confined masonry, tie-columns do not represent the load-bearing part of a structure. The in-plane response of a confined masonry wall is distinctly different from that of reinforced concrete infilled frames, where the frame is constructed prior to the masonry infill. Although a confined masonry wall experiences both flexural and shearing deformations, the masonry infill deforms in a shear mode within a frame that attempts to deform in flexural mode, resulting in separation of the frame and infill wall along the interface.

If properly constructed, confined masonry construction is expected to show satisfactory performance in earthquakes. The bad experience with this form of construction in past earthquakes involved structures that were built without tie columns and/or tie beams, with inadequate roof-to-wall connection, or with poor-quality materials and construction. The main observed damage patterns can be summarized as: (1) shear cracks in walls that propagate into the tie-columns; most cracks passed through mortar joints [5,6], (2) crushing of masonry units has been observed in the middle portion of the walls subjected to maximum stresses, (3) horizontal cracks at the joints between masonry walls and reinforced concrete floors or foundations [7,8], (4) cracks in window piers and walls due to out-of-plane action in inadequately braced walls, (5) crushing of concrete at the joints between vertical tie-columns and horizontal tie beams when the reinforcement was not properly anchored [9,10].

Since 2010, an extensive research program, aiming at developing structurally and economically efficient hybrid building system for developing countries in general and for Egypt in particular, is being undertaken at the Department of Structural Engineering of Ain Shams University. This paper presents the findings of the experimental and analytical phases of this research program on wall assemblies designed and built using locally available materials and with common workmanship and construction practices.

Experimental program

Description of the tested walls

A total of six wall panels were tested in this experimental program. All the panels had an aspect ratio of 1.00 and built with near full-scale dimensions. Fig. 1 shows the dimensions and reinforcement details of typical wall panels, i.e., solid and perforated walls. Table 1 summarizes the various design parameters of the tested panels. Variations include the type of panel (solid, window and door openings), type of used brick (cored clay and solid concrete masonry units), and longitudinal and transverse reinforcement ratios in the confining elements. Single Wythe masonry walls were built directly over reinforced concrete footings using bricks with nominal dimensions of $250 \times 120 \times 60$ mm for both the clay and concrete masonry units. The units were laid in running bond using 10-mm mortar joints and a half brick in alternating courses was left intentionally vacant to form a toothed interlocking connection with the confining columns. Reinforced concrete columns and beams, having rectangular cross-sections of dimensions 120×250 mm, were cast against the brick wall and side timber formwork. Fig. 2a through 2d summarizes the construction sequence of the walls.

For control purposes, standard concrete cubes were cast alongside the walls and were tested at the same day as the tie beams, in order to provide values of the 28-day concrete characteristic compressive strength, (f_{cu}), which was on average 25 MPa. Standard five-brick masonry prisms were built next to the walls and tested at the same day of the wall testing. The mean compressive strength of the clay masonry prisms (f'_m) was 4.5 MPa. The main reinforcement of all confining elements was made of deformed steel bars (Grade 36/52) of nominal yield stress (f_y) of 360 MPa, and ultimate tensile strength (f_u) of 520 MPa. The transverse reinforcement was made of mild steel smooth bars (Grade 24/35) of nominal yield stress (f_y) of 240 MPa, and ultimate tensile strength (f_u) of 350 MPa. All the previous reinforcements had a modulus of elasticity (E_s) of 200 GPa. The walls were left to cure for 28 days before testing and were white washed with non-latex paint to ease the visualization of the developed cracks during testing.

Test setup, boundary conditions and loading scheme

The walls were monotonically tested up to failure under a combination of vertical and monotonically increasing lateral loads. Fig. 3 shows the test setup of the walls. In this respect, a single concentrated load of 150 kN was firstly distributed by a stiff steel distributor I-beam laid on top of secondary steel beams and separated by four rolling steel cylinders as shown in Fig. 3. The secondary beams were laid on top of the concrete tie beam of the wall assembly using gypsum bedding to avoid stress concentration. The purpose of the rolling cylinders is to allow the wall to displace laterally while maintaining the distributed vertical load. The load was chosen to simulate that of a typical module in a two-story residential building with commonly used module dimensions. The lateral load was applied to the tie beam using a 500 kN hydraulic jack. A thick steel plate was placed between the jack and the beam to avoid stress concentration at the loading point. The footing was held in place using two sets of steel struts, the first (Strut A) being horizontal and reacting against the loading frame column to prevent the wall sliding and the second (Strut B) being inclined and reacting against the opposite column to restrain the footing uplift at the loading side. The loading procedure comprised of one loading cycle, during which the load was incrementally increased by 20 kN up to failure. At the end of each load step, the load was held constant for a period of two minutes, during which measurements and marking of cracks took place.

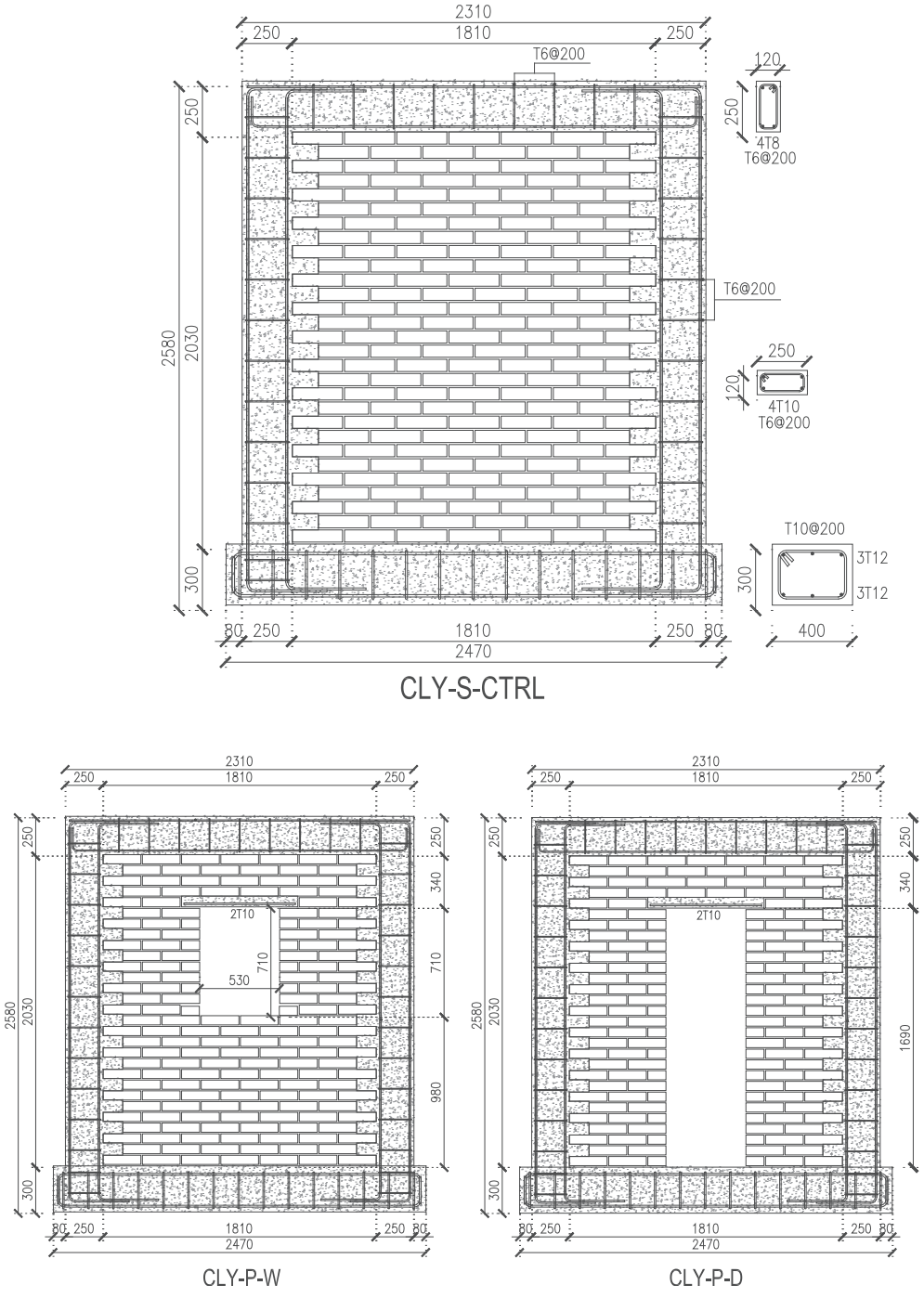

Fig. 1 Typical details of tested walls.

Table 1 Summary of tested walls' design parameters.

Wall ID	Panel type	Brick type	Column longitudinal Rft.	Column Rft. %	Column transverse Rft.
CLY-S-CTRL	Solid	Clay	4 T 10	1.00	T 6 @ 200 mm
CLY-S-L	Solid	Clay	4 T 12	1.50	T 6 @ 200 mm
CLY-S-T	Solid	Clay	4 T 10	1.00	T 6 @ 100 mm
CMU-S	Solid	CMU	4 T 10	1.00	T 6 @ 200 mm
CLY-P-W	Window	Clay	4 T 10	1.00	T 6 @ 200 mm
CLY-P-D	Door	Clay	4 T 10	1.00	T 6 @ 200 mm

Fig. 2 Construction sequence of the wall assemblies.

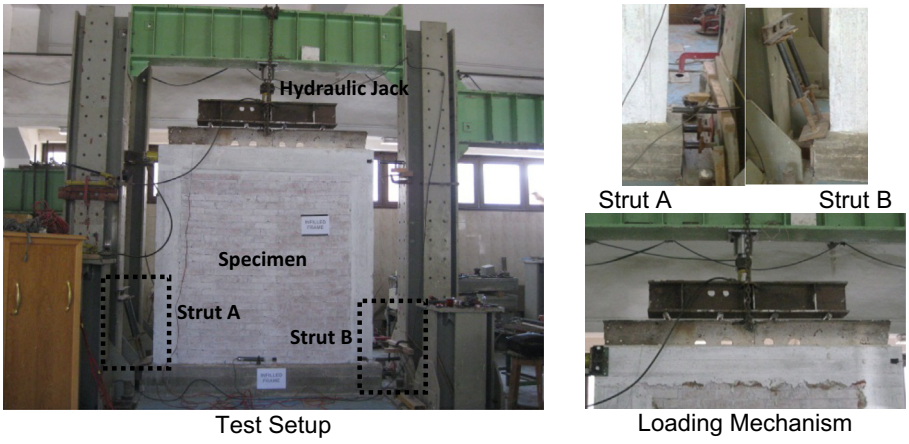

Fig. 3 Test setup, boundary conditions and loading mechanism.

Instrumentation

Measurements were made thoroughly for displacements, steel and concrete strains at key locations of the tested walls. Crack propagation and widths were also monitored during the tests. In this respect, displacements were measured using four 0.01 mm accuracy electrical linear variable distance transducers (LVDTs), coded D1 to D4, positioned as shown in Fig. 4. The steel strain in the longitudinal and transverse reinforcement was monitored using seven electrical strain gauges of 10 mm gauge length and 120 Ohm resistance, coded S1 to S7, as shown in Fig. 4. All previous LVDTs and strain gauges were connected to a computer controlled data acquisition system. The crack pattern was monitored and printed on the walls with the associated load level printed next to it.

Experimental observations and crack patterns

Failure pattern

In general all the wall specimens were tested up to failure which was mainly characterized by discrete stepped bed-joint cracking in the masonry panel in addition to shear failure of the confining columns. Fig. 5a through 5f shows the failure pattern of the tested walls and Table 2 summarizes the key measured response parameters.

Behavior of the tested wall assemblies

The solid wall assemblies with clay bricks (CLY-S-STRL) and concrete masonry units (CMU-S) failed in almost the same

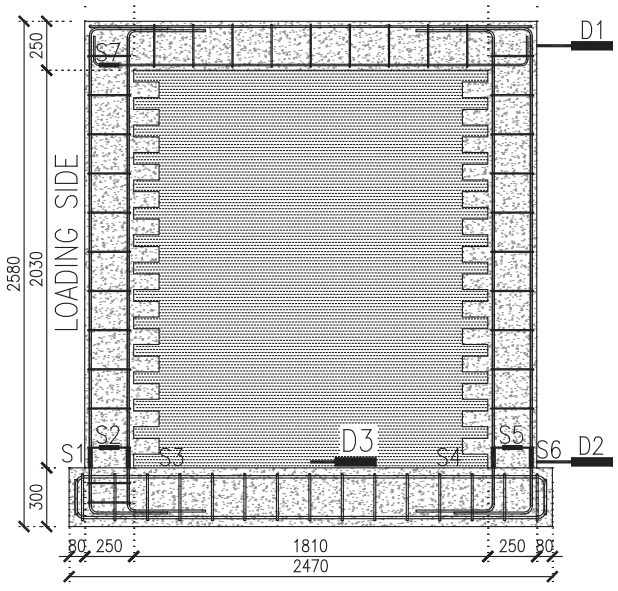

Fig. 4 Instrumentation scheme.

mode, characterized by one diagonal compression strut forming between the top loading corner and the bottom opposing corner. The strut failed due to the transversal tension field by the formation of discrete diagonal bed-joint cracking leading eventually to a diagonal shear failure at the ends of the confining columns. The concrete masonry panel was capable of supporting a higher lateral load of 280 kN compared to 230 kN for the clay masonry panel at about 22% increase in load capacity and 39.50% increase in the displacement capacity. This is mainly attributed to higher strength of the concrete masonry panel.

Walls assemblies (CLY-S-L and CLY-S-T) were solid clay panels with higher longitudinal and transverse reinforcement ratios for the confining columns. Both assemblies failed in a similar fashion as the solid clay control specimen but with significantly wider compression struts in the masonry panel. The recorded ultimate loads were 310 kN and 290 kN for CLY-S-Land CLY-S-T assemblies, respectively, as opposed to 230 kN for the reference control wall (CLY-S-CTRL). These correspond to 34% and 26% increase in the lateral load resistance of the assemblies. The displacement at ultimate load for the CLY-S-L assembly increased by 18.30% and the CLY-S-T assembly increased by 24.75% compared to the solid clay control assembly. These results clearly highlight the importance of the confining columns in maintaining the masonry panel integrity and increasing the load carrying capacity by delaying the eventual shear failure of the columns (see Table 3).

Walls assemblies (CLY-P-W and CLY-P-D) were made with window and door openings, respectively. The window assembly failed by a wide bottle shaped strut formed around

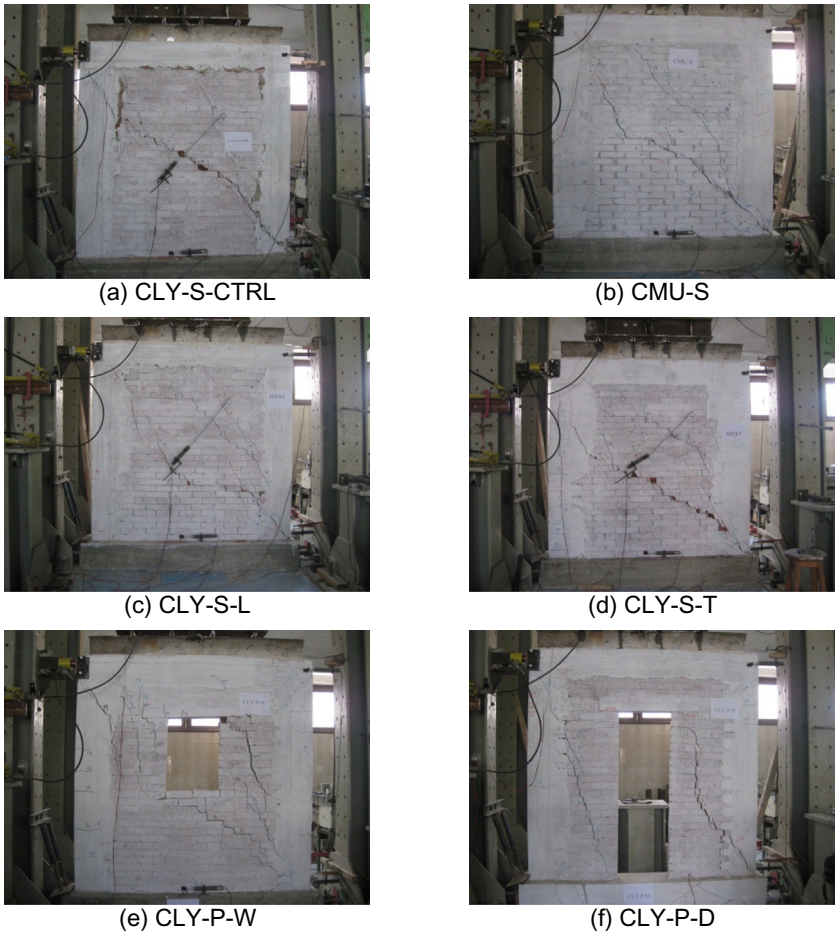

Fig. 5 Failure pattern of the tested assemblies.

Table 2 Summary of tested walls results.

Wall ID	First cracking load (kN)	Maximum load (kN)	Displacement at max. load (mm)
CLY-S-CTRL	200	230	22.25
CLY-S-L	160	310	36.44
CLY-S-T	200	290	38.40
CMU-S	140	280	42.94
CLY-P-W	100	190	24.89
CLY-P-D	100	130	18.51

Table 3 Mohr–Coulomb parameters for concrete and masonry.

Property	Concrete model	Masonry model
Compressive strength	18 MPa	4.5 MPa
Tensile strength	2.55 MPa	0.45 MPa
Cohesive yield stress	3.387 MPa	0.7115 MPa
Friction angle	48.75°	54.9°
Dilation angle	36.1°	16.67°

and encompassing the window opening and leasing to the eventual shear failure of the confining columns. As for the door assembly, a diagonal crack formed at the ends of the door lintel making it to act as a hinged coupling beam and the two door piers responding independently. The piers failed by a steep diagonal crack forming between the two opposing corners as shown in Fig. 5f. The recorded ultimate loads were 190 kN and 130 kN for window and door assemblies, respectively, as opposed to 230 kN for the reference control wall (CLY-S-CTRL). These correspond to 17% and 43% decrease in the lateral load resistance of the assemblies. The displacement at ultimate load for the window assembly increased by 10.6% however the door assembly decreased by 17.7% compared to the solid clay assembly.

Figs. 6a and b show the lateral load vs. the top and base wall displacement curves for all the tested walls, respectively. The figures clearly highlight the brittle nature of this form of construction, where the response is almost linear up to the ultimate load carrying capacity after which the sudden development of columns' shear cracks takes place. This in turn results in a rapid degradation in the strength and stiffness of the wall assembly. Fig. 6a clearly highlights the adverse effect of perforations on the lateral load carrying capacity as well

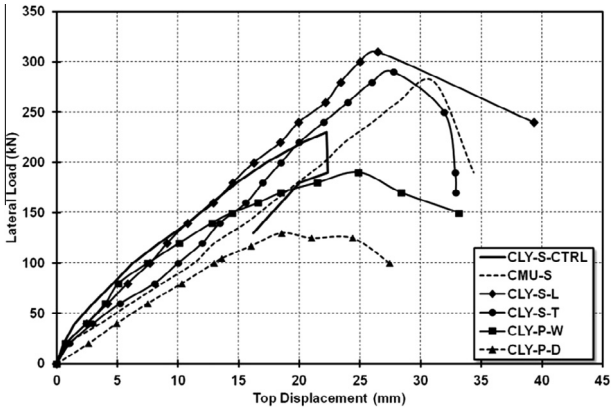

Fig. 6a Lateral load vs. top displacement (D1).

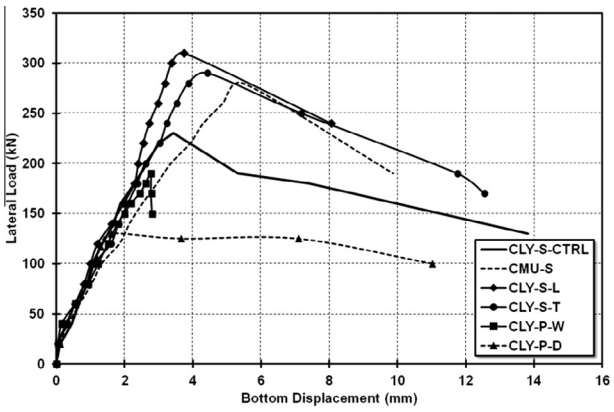

Fig. 6b Lateral load vs. base displacement (D2).

displacement ductility. Increasing the reinforcement ratio for the longitudinal and transverse reinforcements in the confining columns results in a noticeable increase in both aspects of the response, namely lateral load carrying capacity and displacement ductility. Fig. 6b shows that up to the formation of the shear cracks the amount of base sliding is limited which in turn increases rapidly after the formation of the columns' shear cracks.

Numerical simulation of confined masonry walls

The finite element method gives the opportunity to study the wall specimens more thoroughly because of the large amount of results that can be analyzed. Hence, FE-analyses give the possibility to understand how and not just that, a parameter affects the results. This means that the need for experiments can be greatly reduced by using the finite element method. However, the experiments are still needed to verify that the FE-analyses correspond to the actual behavior. Accordingly, when experiments and non-linear finite element analyses are used together they can become very powerful tools in gaining a better understanding of the structural behavior of confined masonry walls under lateral load. In this respect, detailed finite element analyses of the wall specimens have been conducted using the nonlinear finite element program, ABAQUS/Standard 6.9.3 (henceforth referred to as ABAQUS).

Model characterization

The aim of this section is to establish a simple three-dimensional nonlinear model for the tested wall assemblies that are capable of capturing the key response features of this brittle form of construction. The model employed (1) element C3D8, which is a linear 8-node solid element for concrete and masonry elements, and (2) element T3D2 a linear 2-node 3D-truss element for the steel rebars as shown in Fig. 7. The elements were connected together with appropriate constraints to represent the interaction between various components of the wall assembly. In this respect, to simulate the bond between concrete and reinforcement, the reinforcement was embedded in the concrete using the "Embedded Constraint" option in Abaqus, which enforces full compatibility was used which assumes full bond. The interface between the masonry panel and the concrete frame was modeled as a "hard contact" for the normal direction and frictional in the tangential direction

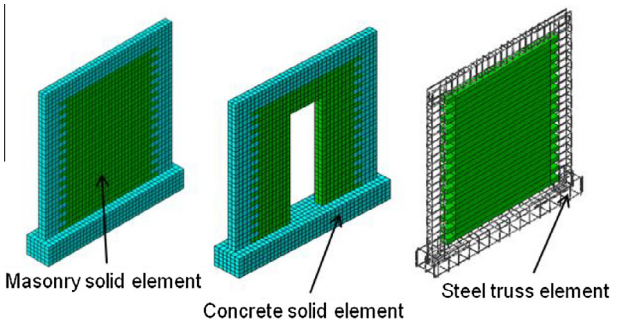

Fig. 7 Element mesh of walls.

with a coefficient of friction of 0.5, as shown in Fig. 8. Fig. 9 shows the boundary conditions for the three-dimensional models. The base of the concrete footing had locked translational degrees of freedom in all directions. The loading of the model was similar to that conducted in the experimental program, where a uniform vertical pressure of 0.50 MPa and an incremental horizontal pressure of 20 MPa for each loading step were applied to the top of the confining column.

Material models

The Mohr–Coulomb failure or strength criterion has been widely used for concrete and masonry. The Mohr–Coulomb criterion assumes that failure occurs when the shear stress on any point in a material reaches a value that depends linearly on the normal stress in the same plane. It assumes that failure is controlled by the maximum shear stress and that this failure shear stress depends on the normal stress.

The material model used for steel reinforcement employs a uni-directional elastic-strain hardening response. The parameters to define this response are yield stress, (f_y) of 360 Pa for 10 and 12 mm bars and (f_y) of 240 MPa for 6 and 8 mm bars and elastic modulus (E_s) of 200 GPa.

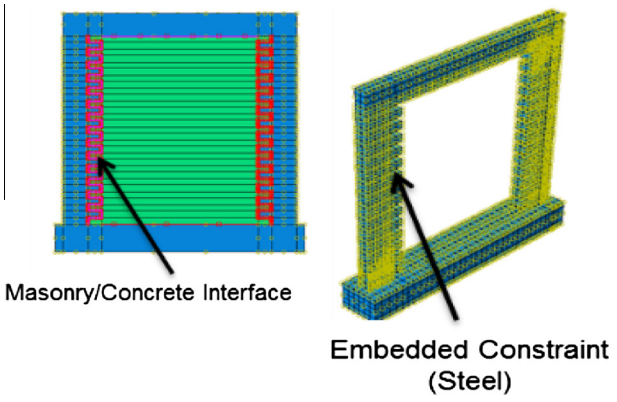

Fig. 8 Interface and constraints for walls.

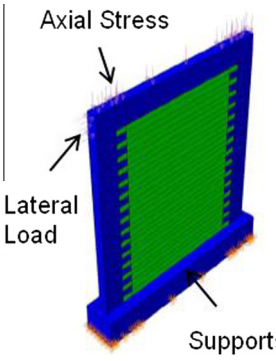

Fig. 9 Boundary conditions and loads.

Model verification

The predicted lateral load capacity and failure mode obtained from the model was examined against the test results for each wall specimens. Fig. 10a shows the load versus top wall displacement from the test and the finite element model for the solid wall panels (CLY-S-CTRL). The difference was 10.9% in ultimate lateral capacity and 20.6% in ultimate lateral displacement for the specimen. Fig. 10b shows the load versus top wall displacement from the test and the finite element model for the wall panel with window opening (CLY-P-W). The difference was 9.2% in ultimate lateral capacity and 12.4% in ultimate lateral displacement for the perforated wall with window opening. Fig. 10c shows the load versus top wall displacement from the test and the finite element model for the wall panel with door opening (CLY-P-D). The difference was 9.6% in ultimate lateral capacity and 17.8% in ultimate lateral displacement for the perforated wall with door opening. Fig. 10d shows the load versus top wall displacement from the test and the finite element model for the solid wall panel with increasing of longitudinal steel (CLY-S-L). The difference was 24.7% in ultimate lateral capacity and 3.2% in ultimate lateral displacement for the solid wall with increase in longitudinal steel in tie columns. Walls' results (ultimate lateral load and ultimate lateral displacement) are summarized as shown in Table 4. Results from the finite element analysis of showed that the developed models are capable with sufficient degree of accuracy to capture the ultimate load and deformation capacity of the tested walls. Though the models exhibit a slightly stiff response in the beginning of the loading, which may be attributed to the smeared nature of the model, the model is considered satisfactory for capturing the global response and ultimate capacities of the walls. The degree of simplification in modeling is considered acceptable given the brittle nature of the response of CM walls.

Parametric study using FE models

It can be seen from the verification stage in the previous section, that the FE-models capture the structural behavior of the tested wall specimens in a satisfactory way. There are a lot of parameters that are believed to affect the lateral load capacity of confined masonry walls. The parameters are the amount of longitudinal steel in tie columns, number of tie columns, effect of tie columns around opening, width of opening for both walls with window and door openings, aspect ratio effect and axial stresses. The developed model will be used in this section to further investigate and evaluate these parameters.

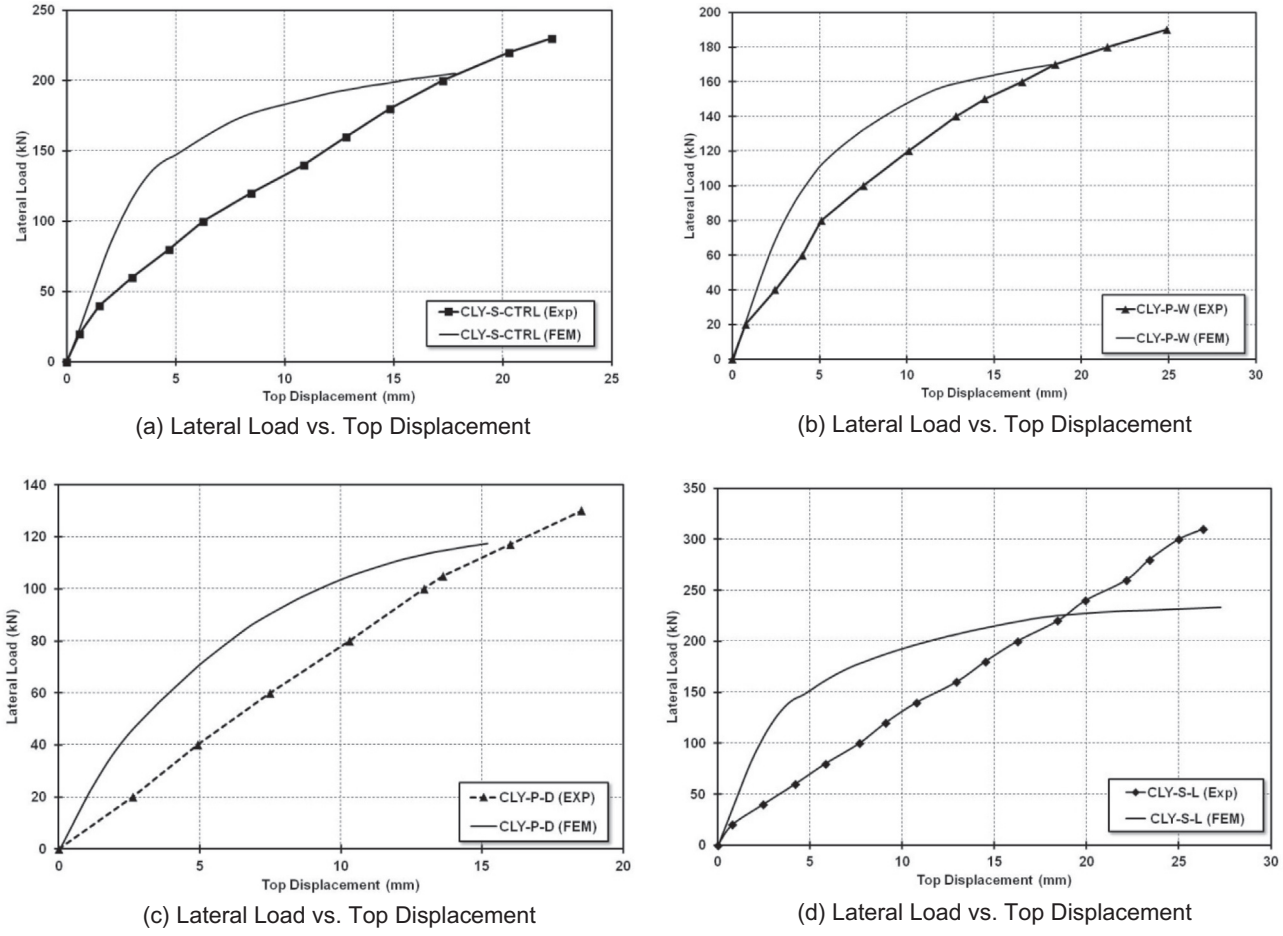

(a) Lateral Load vs. Top Displacement

(b) Lateral Load vs. Top Displacement

(c) Lateral Load vs. Top Displacement

(d) Lateral Load vs. Top Displacement

Fig. 10 Load vs. lateral displacement for wall assemblies (test vs. FEM).

Table 4 Summary of model vs. test comparison.

Wall ID	Ultimate load (kN)			Displacement at max. load (mm)		
	Exp.	Num.	Exp./Num.	Exp.	Num.	Exp./Num.
CLY-S-CTRL	230	204.9	1.12	22.25	17.44	1.29
CLY-P-W	190	172.54	1.10	24.89	21.78	1.14
CLY-P-D	130	117.48	1.11	18.51	15.19	1.22
CLY-S-L	310	233.46	1.33	26.44	27.27	0.97
CLY-S-T	290	193.5	1.50	27.76	14.1	1.97

Table 5 Tested wall assemblies and results.

Wall ID	Wall type	Column longitudinal Rft.	Column Rft. %	Ultimate load (kN)	% Load difference	Displacement at max. load (mm)
CLY-S-4T8	Solid	4 T 8	0.67	190.52	−7	23.42
CLY-S-4T10	Solid	4 T 10	1.00	204.91	–	17.44
CLY-S-4T12	Solid	4 T 12	1.50	233.46	13.9	27.27
CLY-P-W-4T8	Window	4 T 8	0.67	159.50	−7.55	20.23
CLY-P-W-4T10	Window	4 T 10	1.00	172.54	–	21.78
CLY-P-W-4T12	Window	4 T 12	1.50	184.45	6.9	21.02
CLY-P-D-4T8	Door	4 T 8	0.67	113.82	−3	19.31
CLY-P-D-4T10	Door	4 T 10	1.00	117.42	–	15.19
CLY-P-D-4T12	Door	4 T 12	1.50	123.36	5	15.79

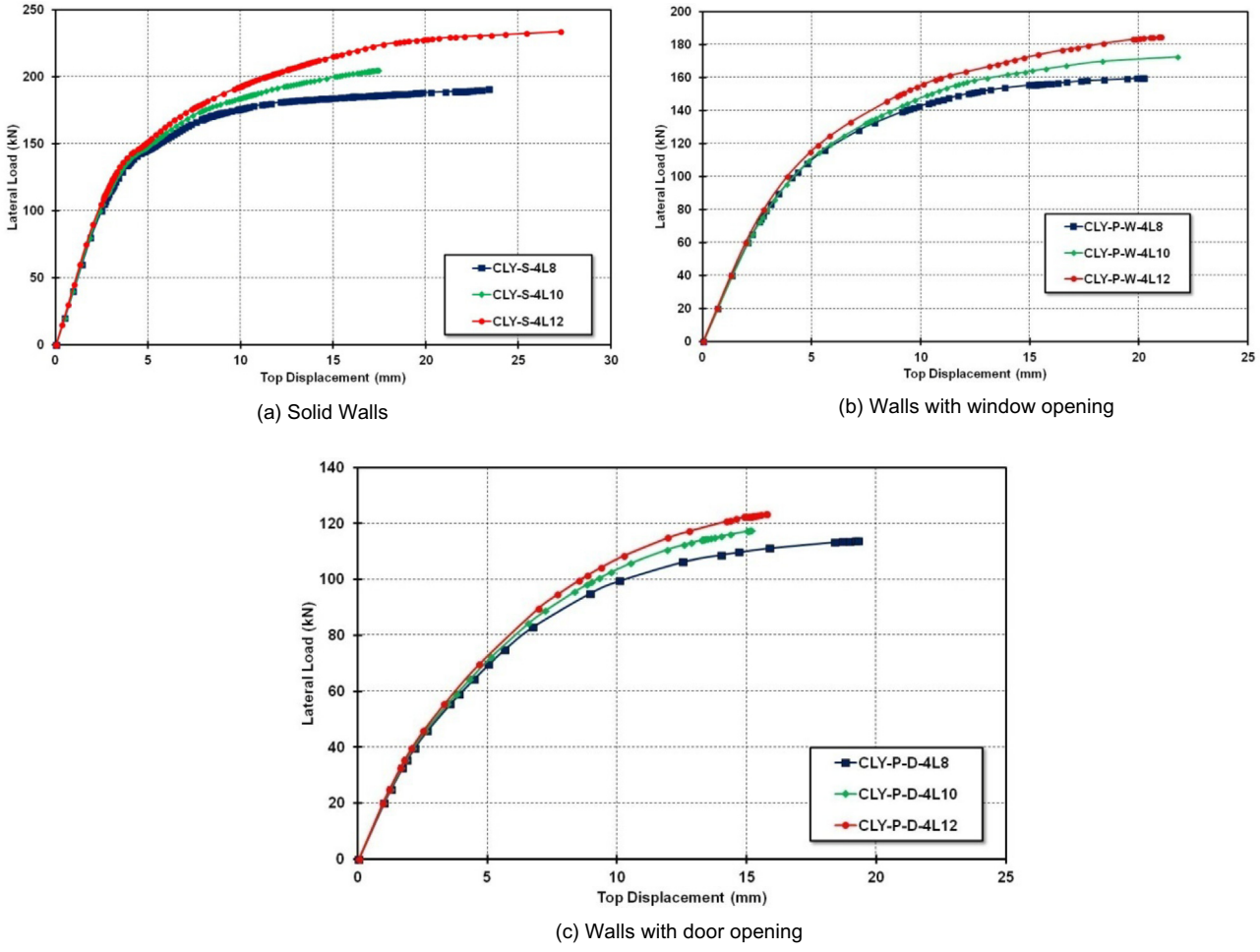

Fig. 11 Lateral load vs. top displacement.

Table 6 Tested wall assemblies and results.

Wall ID	Wall type	No. of tie columns	Ultimate load (kN)	% Load increase	Displacement at max. load (mm)
CLY-S-AR0.5-2TC	Solid	Two	408.93	–	28.55
CLY-S-AR0.5-3TC	Solid	Three	542.92	33	42.80
CLY-S-AR0.5-4TC	Solid	Four	680.64	66	50.59
CLY-S-AR0.5-5TC	Solid	Five	782.91	91	47.62
CLY-P-W-AR0.5-2TC	Window	Two	352.06	–	23.44
CLY-P-W-AR0.5-4TC	Window	Four	443.74	26	20.47
CLY-P-D-AR0.5-2TC	Door	Two	253.67	–	8.70
CLY-P-D-AR0.5-4TC	Door	Four	365.92	44	16.39
CLY-P-2W-AR0.5-2TC	Two Window	Two	306.24	–	27.78
CLY-P-2W-AR0.5-3TC	Two Window	Three	386.60	26	24.39
CLY-P-2D-AR0.5-2TC	Two Door	Two	208.18	–	72.64
CLY-P-2D-AR0.5-3TC	Two Door	Three	266.68	28	16.80
CLY-P-WD-AR0.5-2TC	Window & Door	Two	211.13	–	12.19
CLY-P-WD-AR0.5-3TC	Window & Door	Three	308.72	46	20.74
CLY-P-DW-AR0.5-2TC	Door & Window	Two	280.00	–	27.75
CLY-P-DW-AR0.5-3TC	Door & Window	Three	370.31	32	35.76

Longitudinal reinforcement in tie columns

Additional walls were analyzed to extend results and study the effect of main steel amount in tie columns on lateral load capacity of both solid walls and openings walls as well as ultimate displacement capacity. Tested walls were same in the other parameters such as dimensions of specimen, vertical stress and brick type and aspect ratio $(h/l) = 1$. Table 5 presents a summary of the lateral load capacity and maximum displacement as well as the percentage difference over the

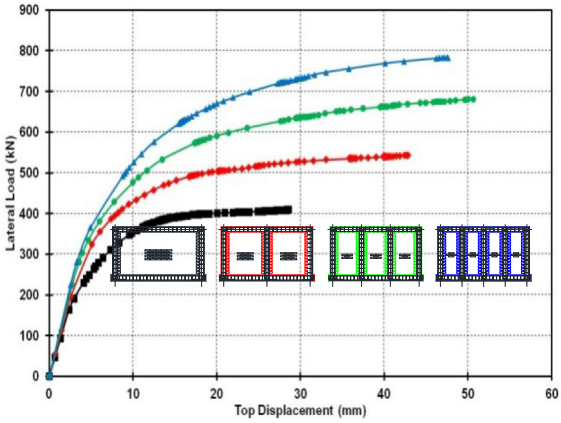

(a) Solid Walls

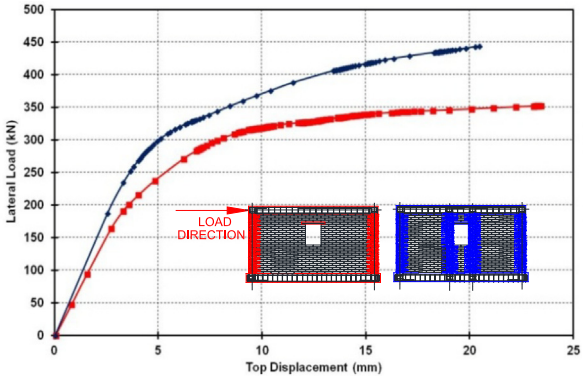

(b) Walls with Window Opening

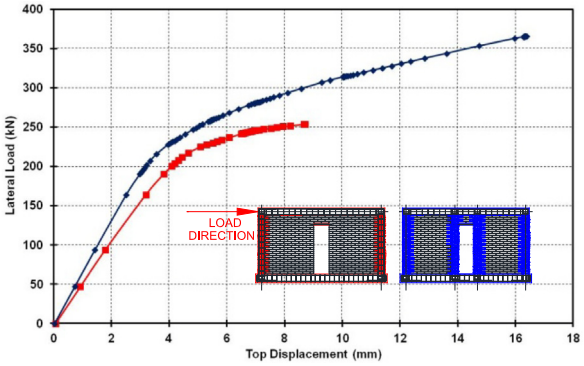

(c) Walls with Door Opening

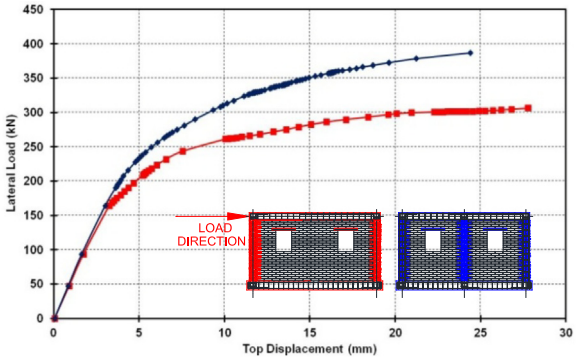

(d) Walls with two Window Opening

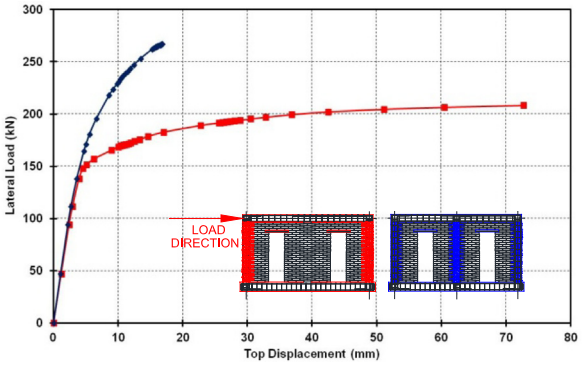

(e) Walls with two Door Opening

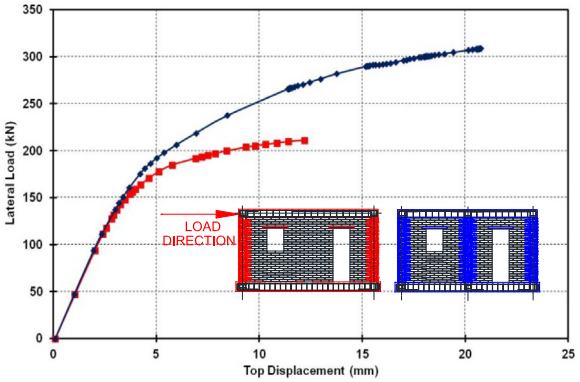

(f) Walls with Window and Door Opening

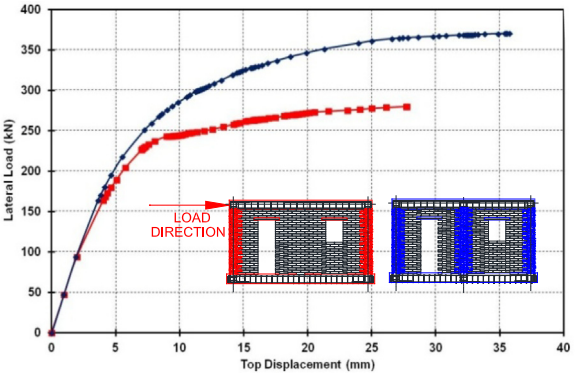

(g) Walls with Door and Window Opening

Fig. 12 Lateral load vs. top displacement.

Fig. 13 Tested CM walls.

walls. Two models were added to every assembly type (solid wall, window opening wall and door opening wall). Fig. 11a through Fig. 11c shows the lateral load versus top lateral displacement relationships form FE analysis in comparison to the corresponding studied walls.

Tie columns effect

Effect of tie columns on lateral load capacity was studied also in solid walls, window opening walls and door opening walls. Table 6 shows the configuration assemblies and presents a summary of the lateral load capacity and maximum displacement as well as the percentage difference over the walls. Number of tie columns was increased from two through five in four solid assemblies with the same parameters and aspect ratio 0.5. Fig. 12a shows the relation of lateral load capacity as well as ultimate displacement capacity. Fig. 12b through 12g shows the lateral load capacity as well as ultimate displacement capacity for the perforated assemblies with single and double openings door or/and window.

Width of opening

Width of opening was studied in window openings walls and door opening walls with the same parameters such as dimensions of specimen, vertical stress and brick type. Aspect ratio

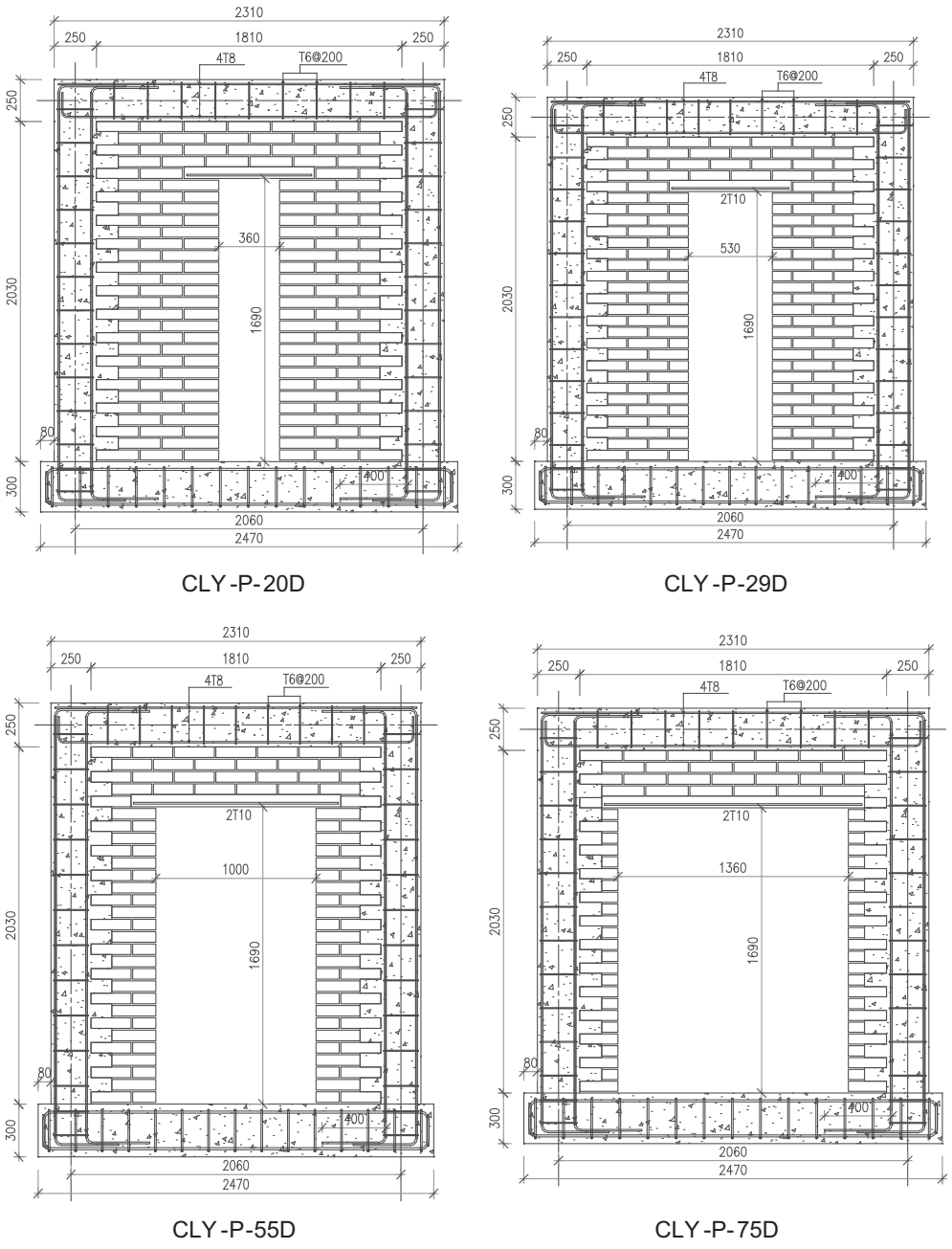

Fig 13. *(continued)*

(h/l) was 1 for these specimens as shown in Fig. 13. Table 7 shows the details of walls and the results of ultimate load and displacement. Load displacement comparison between the specimens is mentioned in curves as shown in Fig. 14.

Opening positions in CM panel walls

The opening positions in CM walls were studied in window openings walls and door opening walls with the same parameters such as dimensions of specimen, vertical stress and brick type. And Aspect ratio (h/l) = 1 for these specimens, details and results as shown in Table 8. Load displacement compassion between the three types of specimens is mentioned in curves as shown in Fig. 15.

Axial stress effect

Finite element models were analyzed with different axial stress for walls with window opening. Assemblies (CLY-P-W-ST0.5) and (CLY-P-W-ST1) were effected with axial stress 0.50 MPa and 1.00 MPa, respectively. The wall's ultimate loads were 168 kN and 204 kN. This means lateral load resistance of the wall increases to 21% when the axial stress increases to 1.00 MPa. Furthermore the displacement at ultimate load

Table 7 Tested wall assemblies and results.

Wall ID	Wall type	% Width of opening	Ultimate load (kN)	% Load decrease	Displacement at max. load (mm)
CLY-P-20W	Window	0.20	190.76	–	23.97
CLY-P-29W	Window	0.29	172.54	9.55	21.78
CLY-P-55W	Window	0.55	154.81	18.85	65.53
CLY-P-75W	Window	0.75	136	28.7	85.55
CLY-P-20D	Door	0.20	128.90	–	9.88
CLY-P-29D	Door	0.29	117.48	8.86	15.19
CLY-P-55D	Door	0.55	116.89	9.32	113.25
CLY-P-75D	Door	0.75	97.95	24	194.47

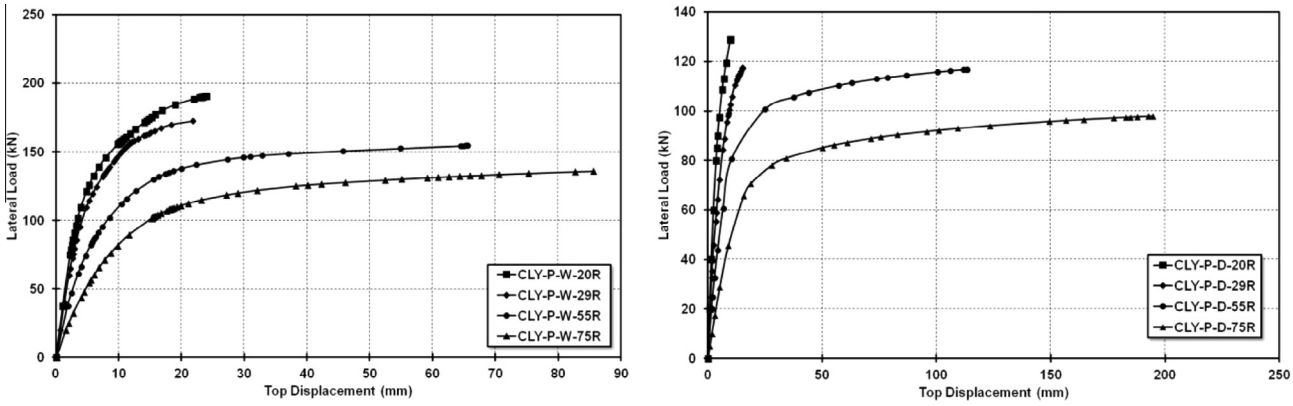

Fig. 14 Lateral load vs. top displacement.

Table 8 Tested wall assemblies and results.

Wall ID	Wall type	Column longitudinal Rft.	Column Rft.%	Ultimate load (kN)	% Load increase	Displacement at max. load (mm)
CLY-P-W	Window	4 T 10	1.00%	168.6	–	18.3
CLY-P-W-LEFT	Window	4 T 10	1.00%	176.7	4.8	23
CLY-P-W-RIGHT	Window	4 T 10	1.00%	155.9	−7.53	14.8
CLY-P-D	Door	4 T 10	1.00%	118.2	–	17.8
CLY-P-D-LEFT	Door	4 T 10	1.00%	161.5	36.63	19.5
CLY-P-D-RIGHT	Door	4 T 10	1.00%	145.9	23.43	12.5

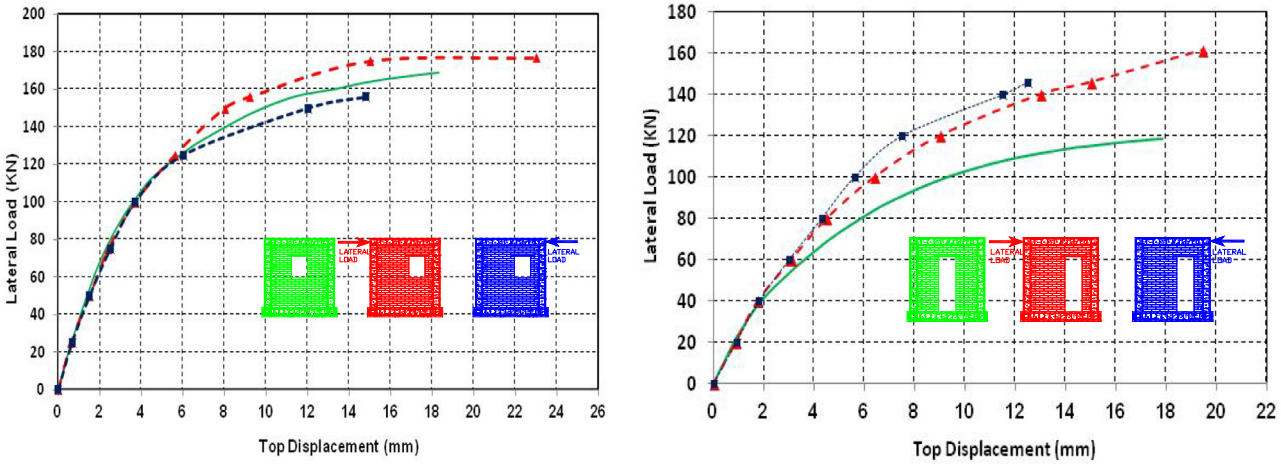

Fig. 15 Lateral load vs. top displacement.

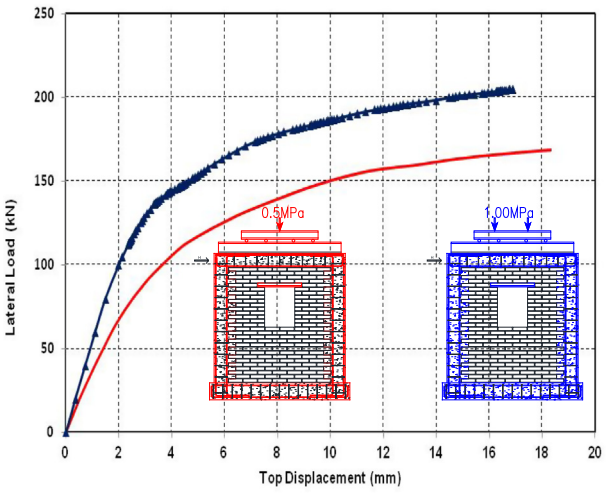

Fig. 16 Lateral load vs. top displacement.

decreased with a factor of about 8.2% as shown in the lateral load versus top wall displacement curves in Fig. 16.

Conclusions

This paper presents an experimental–analytical investigation of the lateral load response of confined masonry walls built using Egyptian materials and workmanship. The findings of the research programs resulted in the following conclusions:

1. Higher strength bricks as in the case of concrete masonry units result in a considerable increase in the lateral load capacity of the walls.
2. Confining elements play an important role in maintaining the strength and ductility of the confined walls, higher reinforcement ratios and increased number of confining elements provide the wall with significant strength reserve.
3. The lateral load capacity is inversely proportional to the width of the perforations in the wall whether it is a door or a window opening. Confining the openings with tie columns helps restore the reduced capacity and significantly enhance the wall ductility.
4. Higher aspect ratios drive the wall into a flexure dominated failure mode and consequently enhance the strength and ductility of the walls.
5. Due to diagonal tension failure mode of squat panels, increasing the axial load will result in a considerable increase in the lateral load carrying capacity of the wall assembly.

Conflict of interest

None declared.

References

[1] S.M. Alcocer, J.G. Arias, A. Vazquez, The new Mexico City building code requirements for design and construction of masonry structures, in: The proceedings of the Ninth North American Masonry Conference, Clemson, South Carolina, 2003, pp. 656–667.
[2] S.M. Alcocer, J.G. Arias, A. Vazquez, Response assessment of Mexican confined masonry structures through shaking table tests, in: 13th world conference on earthquake engineering, Vancouver, B.C., Canada, 2004, No. 2130.
[3] S.M. Alcocer, R. Meli, Experimental program on the seismic behaviour of confined masonry structures, in: Proceedings of the sixth North American masonry conference, Philadelphia, vol 2, 1993.
[4] G. Aguilar, R. Meli, R. Diaz, Influence of horizontal reinforcement on the behaviour of confined masonry walls, in: 11th World Conference on Earthquake Engineering, Acapulco, Mexico, 1996, No 1380.
[5] S.M. Alcocer, C. Reyes, D. Bitran, O. Zepeda, L.E. Flores, M.A. Pacheco, An assessment of the seismic vulnerability of housing in Mexico, in: Proceedings of the 7th US national conference on earthquake engineering, Boston, Massachusetts, 2002.
[6] S.M. Alcocer, Zepeda, Behaviour of multi-perforated clay brick walls under earthquake-type loading, in: 8th North American masonry conference, Austin, Texas, USA, 1999.
[7] J.J. Alvarez, Some topics on the seismic behaviour of confined masonry structures, in: 11th World Conference on Earthquake Engineering, Acapulco, Mexico, 1996, No. 180.
[8] J. Bariola, C. Delgado, Design of confined masonry walls under lateral loading, in: 11th World Conference on Earthquake Engineering, Acapulco, Mexico, 1996, No. 204.
[9] E. Castilla, A. Marinilli, Recent experiments with confined concrete block masonry walls, in: 12th international Brick/block masonry conference, Amsterdam, Netherlands, 2000, pp. 419–431.
[10] M.A. ElGawady, P. Lestuzzi, M. Badoux, Dynamic tests on URM walls before and after upgrading with composites, Experimental Rep., Publication No. 1, IMAC ENAC, EPFL, Switzerland. European committee for standardization; (2002) European standard.